Suppression of Multiple Spatially Correlated Jammers

Linh Manh Hoang, *Student Member, IEEE*, J. Andrew Zhang, *Senior Member, IEEE*, Diep Nguyen, *Senior Member, IEEE*, Xiaojing Huang, *Senior Member, IEEE*, Asanka Kekirigoda, and Kin-Ping Hui

***Abstract*—Effective suppression of inadvertent or deliberate jamming signals is crucial to ensure reliable wireless communication. However, as demonstrated in this paper, when the transmitted jamming signals are highly correlated, and especially when the correlation coefficient varies, nullifying the jamming signals can be challenging. Unlike existing techniques that often assume uncorrelated jamming signals or non-zero but constant correlation, we analyze the impact of the non-zero and varying correlations between transmitted jamming signals on the suppression of the jamming signals. Specifically, we observe that by varying the correlation coefficients between transmitted jamming signals, jammers can "virtually change" the jamming channels hence their nullspace, even when these channels do not physically change. This makes most jamming suppression techniques that rely on steering receiving beams towards the nullspace of jamming channels no longer applicable. To tackle the problem, we develop techniques to effectively track the jamming nullspace and correspondingly update receiving beams. Monte Carlo simulations show that our proposed techniques can suppress/nullify jamming signals for all considered scenarios with non-zero and varying correlation coefficients amongst transmitted jamming signals.**

***Index Terms*—Jamming suppression, multi-user MIMO, correlated jamming.**

I. Introduction

Wireless communication is particularly susceptible to radio-frequency (RF) jamming, which either inadvertently or deliberately disrupts the signal reception/decoding. Among different types of jammers, the proactive type is the most popular due to its simplicity [1]. A smart jammer is capable of designing the jamming signals to counteract jamming suppression techniques, which makes jamming suppression more challenging.

One conventional approach for suppressing jamming is nullifying jamming signals using the angle of arrival (AOA) based beam-forming technique. It is realized by steering the nulls in the receiving beam towards the AOAs of jamming signals, which are obtained by AOA estimation techniques [2]. Popular examples of such an approach are multiple signal classification (MUSIC) [3], estimation of signal parameters via rotational invariance techniques (ESPRIT) [4], and the matrix pencil [5]. However, for these techniques, the receiver has to "sacrifice" at least one antenna to nullify each arriving jamming signal [6]. This makes the approach not suitable when the number of jammers is large, or when the signal from each jammer reaches the receiver through a large number of propagation paths (e.g., in the urban areas). This is because the receiver does not want to "lose" too many antennas for jamming suppression, as a lower number of remaining antennas generally results in a lower or even zero throughputs between legitimate devices [7].

Alternatively, jamming suppression can be realized by estimating the projection of jamming channels [8]–[10], the ratios between jamming channels [11], or the nullspace of the jamming channels [12]–[16], and then designing filters to nullify the jamming signals. The jamming rejection combining (IRC) technique [17] considers the impact of the correlations between jamming channels on jamming suppression performance. These methods require only one receiver's antennas to nullify each spatial stream of a jammer, which is more effective than the AOA based beam-forming technique mentioned above.

However, the techniques in [8]–[17] do not consider the impact of the correlations between transmitted jamming signals on the jamming nullification performance. Note that the correlation between the jamming channels does not affect the estimation of the jamming channels' nullspace. On the other hand, the correlations between transmitted jamming signals, as will be demonstrated in this paper, cause a "virtual change" in the jamming channels, making the estimated nullspace incapable in nullifying the jamming signals. Therefore, there exist significant differences between our work and those in [8]–[17]. In [18] and [19], the authors show that, by choosing a suitable correlation, the jammers can maximize the jamming impact to communications between legitimate devices. Therefore, to ensure the effectiveness of jamming suppression techniques, it is important to consider the correlations between transmitted jamming signals. Nonetheless, the main objective of [18] and [19] is to analyze the impact of the correlation on the jamming outcome. The two papers neither propose any suppression technique for correlated jamming nor discusses the impact of the correlation on the performance of such a jamming nullification method, especially under time-varying channels. Another unanswered question is the impact of varying the non-zero correlation coefficient, if any, on the jamming suppression process.

In fact, if ignoring the RF ineffectiveness in sacrificing the

J. A. Zhang, D. Nguyen, and X. Huang's research in this work is partially supported by the Commonwealth of Australia as represented by the Defence Science and Technology Group of the Department of Defence

L. M. Hoang, J. A. Zhang, D. Nguyen, and X. Huang are with the Global Big Data Technologies Centre, University of Technology Sydney, Sydney, Australia (e-mail: Linh.M.Hoang@student.uts.edu.au; Andrew.Zhang@uts.edu.au; Diep.Nguyen@uts.edu.au; Xiaojing.Huang@uts.edu.au).

A. Kekirigoda and K. Hui are with the Defence Science and Technology (DST), Edinburgh, Australia (e-mail: Asanka.Kekirigoda@dst.defence.gov.au; Kinping.Hui@dst.defence.gov.au).

antennas or degree-of-freedom, the AOA based beam-forming technique described above can deal quite well in the cases with non-zero correlations between transmitted jamming signals. Specifically, when the jamming signals are correlated, the spatial smoothing technique [20] can be applied to decorrelate the jamming signals and estimate their AOAs. The spatial smoothing is implemented by dividing the receiver's antenna array into sub-arrays and averaging signals from these sub-arrays. However, as aforementioned, a large number of antennas are required to nullify each spatial stream of a jammer, making the AOA based beam-forming techniques inappropriate when the number of jammers is large, or the signal from each jammer arrives the receiver via multiple independent propagation paths.

The jamming suppression has some analogies to the interference avoidance in cognitive radio. The secondary user (SU) tries to avoid interference with the primary user (PU) by transmitting signals that lie in the nullspace of the channel between SU transmitter and PU receiver. In [21], [22], the authors propose blind nullspace learning and tracking techniques to estimate the nullspace of the channel between the SU transmitter and the PU receiver, without requiring any SU-PU interaction. This is realized by having the SU continuously adjust the transmitted signal's spatial direction and monitor the impact of the adjustment on the interference output on the PU's receiver (by observing the transmitted power from the corresponding PU transmitter). However, this approach cannot be applied in the jamming suppression scenario, because we do not have control over the transmitted signals from malicious jammers.

This paper studies the impact of the non-zero and varying correlations between transmitted jamming signals on the jamming suppression/nullification in a multi-user multiple-input multiple-output (MU-MIMO) system. Although there exist some works on exploiting channel variations to improve frequency diversity [23] and delay diversity [24], our work uniquely aims to combat the artificial channel variation caused by varying correlation of jamming signals. We start with the jamming suppression for uncorrelated jamming signals yet under time-varying channels. We then prove that the effect of non-zero and varying correlations on the jamming suppression process is similar to that under the time-varying channels. This finding then guides us to develop jamming nullification techniques that effectively track the jamming nullspace and correspondingly update receiving beams under all correlation levels. Our proposed techniques cost only a single degree-of-freedom of receiving antennas to nullify each jammers' spatial stream. Monte Carlo simulations are provided, showing that our techniques are capable of suppressing the jamming signals for all considered scenarios with non-zero and varying correlations (between transmitted jamming signals). The contributions of this paper can be summarized as follows.

- Study the impact of the non-zero correlations between transmitted jamming signals on the jamming suppression/nullification process.
- Reveal that by varying the correlation coefficients, jammers can effectively "change" the jamming channels even when these channels do not physically change.

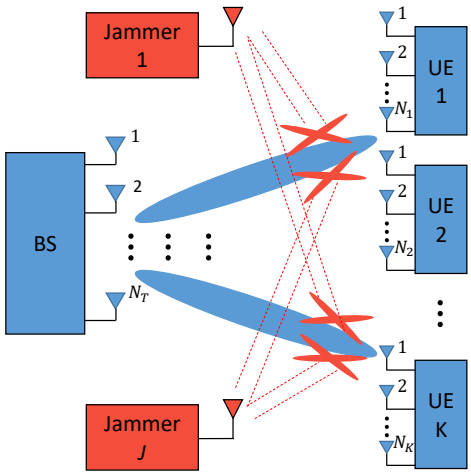

Fig. 1: MU-MIMO system with proactive jammers.

- Characterize the impact of the non-zero and varying correlations on the jamming suppression/nullification process.
- Develop novel jamming suppression algorithms that effectively update the beam-forming matrix to suppress the jamming signals for all considered scenarios with non-zero and varying correlations.
- Propose jamming nullification techniques that cost only one receiver's degree-of-freedom to suppress each spatial stream of the jamming signals, so that the remaining antennas can be used for the communication between legitimate devices.

The remainder of this paper is organized as follows. Section II describes the system model and problem formulation. The impact of the correlations between transmitted jamming signals on nullspace estimation is described in Section III. Section IV considers jamming nullification when the jamming signals are uncorrelated. Section V presents jamming nullification techniques when the correlations are non-zero and varying. Monte Carlo simulation results are provided in Section VI. Finally, conclusions are drawn in Section VII.

II. System Model and Problem Formulation

In this section, we present our scheme by considering a multi-user multiple-input multiple-output (MU-MIMO) downlink system with N_T transmit antennas at the BS and N_k receive antennas at the kth user equipment (UE), as illustrated in Fig. 1. The BS communicates with K UEs using MU-MIMO. The number of independent data streams for the kth UE is D_k. There are N_J single-antenna proactive jammers that interfere with BS-UEs communication by continuously transmitting jamming signals. Note that this paper's techniques are also suitable for multiple-antennas jammers, because a jammer with multiple antennas can be considered multiple single-antenna jammers. For both cases, we assume there are in total N_J jamming antennas from jammers.

The received signals at the kth UE is given by

$$\mathbf{y}_k = \mathbf{H}_k \mathbf{P}_k \mathbf{x}_k + \mathbf{H}_k \sum_{l \neq k}^{K} \mathbf{P}_l \mathbf{x}_l + \mathbf{Z}_k \mathbf{x}_{\mathrm{J}} + \mathbf{n}, \tag{1}$$

where $\mathbf{H}_k \in \mathbb{C}^{N_k \times N_T}$ denotes the channel matrix between the BS and the kth UE, $\mathbf{P}_k \in \mathbb{C}^{N_T \times D_k}$ is the precoding matrix applied at the BS for the kth UE, $\mathbf{x}_k \in \mathbb{C}^{D_k \times 1}$ denotes the transmitted signal from the BS to the kth UE, $\mathbf{Z}_k \in \mathbb{C}^{N_k \times N_J}$ is the channel matrix between N_J jammers and the kth UE, $\mathbf{x}_{\mathrm{J}} = [x_{\mathrm{J}1}; x_{\mathrm{J}2}; ...x_{\mathrm{J}N_J}] \in \mathbb{C}^{N_J \times 1}$ stands for the transmitted jamming signals, and $\mathbf{n} \in \mathbb{C}^{N_k \times 1}$ is complex noise. We assume that the elements of $\mathbf{n}$ are independent and identically distributed (i.i.d.) zero-mean circularly-symmetric complex Gaussian random variables (i.e., $\mathbf{n} \sim \mathcal{CN}(\mathbf{0}, \sigma_n^2 \mathbf{I}_{N_k})$, where $\mathbf{I}_{N_k}$ denotes an identity matrix of size N_k and σ_n^2 is the noise variance). Similarly, $\mathbf{x}_k \sim \mathcal{CN}(\mathbf{0}, \mathbf{\Sigma}_{\mathbf{x}_k})$, where $\mathbf{\Sigma}_{\mathbf{x}_k}$ is the covariance matrix of the transmitted signal from the BS (to the kth UE). For the transmitted jamming signals, we assume that $\mathbf{x}_{\mathrm{J}} \sim \mathcal{CF}(\boldsymbol{\mu}_{\mathrm{J}}, \mathbf{\Sigma}_{\mathrm{J}})$ with $\mathcal{F}$ being an unspecified complex distribution function unknown to the BS and the UEs, $\boldsymbol{\mu}_{\mathrm{J}}$ is the mean, and $\mathbf{\Sigma}_{\mathrm{J}}$ is the covariance matrix of the transmitted jamming signals.. We assume that the jammers, if more than one, can coordinate to control the correlation between the transmitted jamming signals. For ease of reference, important symbols and notations are summarized in Table I. Note that we use superscripts "s", "d", and "i" to represent symbols in the (inter-frame) silent period, data transmission period, and intra-frame silent period, respectively. On the other hand, we use the subscripts "c" and "s" to indicate symbols for the jamming channels and the received jamming signals, respectively.

The channel $\mathbf{H}_k$ from the BS to the kth UE can be written as

$$\mathbf{H}_k = \frac{1}{\sqrt{L_k}} \sum_{p=1}^{P_k} \alpha_k^p \mathbf{a}(\phi_{\mathrm{a},k}^p) \mathbf{a}(\phi_{\mathrm{d},k})^T, \tag{2}$$

where L_k denotes the large-scale path-loss of signal energy transmitted from the BS to the kth UE, α_k^p represents the complex path gain of the pth path, corresponding to the small-scale fading, P_k is the total number of propagation paths, $\mathbf{a}(\phi_{\mathrm{a},k}^p)$ is the steering vector [2] corresponding to the AoA $\phi_{\mathrm{a},k}^p$, which is uniformly distributed over $[0, 2\pi]$ [26], and $\mathbf{a}(\phi_{\mathrm{d},k})$ is the steering vector associated with the angle of departure (AoD) $\phi_{\mathrm{d},k}$ from the BS. Similarly, the channel from the jth jammer to the kth UE can be represented as

$$\mathbf{Z}_{k,j} = \frac{1}{\sqrt{L_{k,j}}} \sum_{p=1}^{P_{k,j}} \alpha_{k,j}^p \mathbf{a}(\phi_{\mathrm{a},k,j}^p), \tag{3}$$

where $L_{k,j}$, $\alpha_{k,j}^p$, $P_{k,j}$, $\mathbf{a}(\phi_{\mathrm{a},k,j}^p)$, and $\phi_{\mathrm{a},k,j}^p$ are defined similarly to those in (2). The path-losses L_k and $L_{k,j}$ are modeled using the COST 231 Hata model [27, p. 135], and the multipath fading (i.e., demonstrated by the summation in (2) and (3)) is modeled using a flat fading Rician channel model from [28]. The detailed values of the parameters are given in the Simulation section.

To guarantee BS-UE communication, both interference signals from other UEs and the jamming signals need to be suppressed. There already exist various techniques for suppressing the interference signals, including orthogonal signal design, precoder, and linear minimum mean square error (LMMSE) equalization. Therefore, in this paper, we concentrate on techniques for suppressing the jamming signals. In particular, in the subspace-based approach, this is achieved by multiplying the received signal with a beam-forming matrix derived from the left nullspace [25, p. 181] of the received jamming signals. The received signal after nullification can be represented as [29],

$$\mathbf{p}_k = \mathbf{W}_k (\mathbf{H}_k \mathbf{P}_k \mathbf{x}_k + \mathbf{H}_k \sum_{l \neq k}^{K} \mathbf{P}_l \mathbf{x}_l + \mathbf{Z}_k \mathbf{x}_{\mathrm{J}} + \mathbf{n}), \tag{4}$$

where $\mathbf{W}_k$ is the beam-forming matrix used to nullify the received jamming signals.

Fig. 2 illustrates a baseline jamming nullification and BS-UE data transmission protocol based on the protocol in [17]. It starts with a silent period, during which the BS does not send any signal, and $\mathbf{Q}_{\mathrm{s}_k}^{\mathrm{s}} \in \mathbb{C}^{(N_k - N_J) \times N_k}$ is estimated for the first time. Note that, as summarized in Table I, $\mathbf{Q}_{\mathrm{s}_k}^{\mathrm{s}}$ denotes the matrix whose rows form an orthonormal basis for the left nullspace of the received jamming signals at the kth UE in the inter-frame silent period. Because the number of jammers N_J can be estimated by using the minimum description length (MDL) method [30], the number of rows of $\mathbf{Q}_{\mathrm{s}_k}^{\mathrm{s}}$ can be determined. The estimated value of $\mathbf{Q}_{\mathrm{s}_k}^{\mathrm{s}}$ is denoted by $\hat{\mathbf{Q}}_{\mathrm{s}_k}^{\mathrm{s}}$.

TABLE I: Summary of symbols and notations.

Notation	Description
$\mathbf{x}_{\mathrm{J}}^{\mathrm{s}}$, $\mathbf{x}_{\mathrm{J}}^{\mathrm{d}}$, $\mathbf{x}_{\mathrm{J}}^{\mathrm{i}}$	Transmitted jamming signals in the inter-frame silent, data transmission, and intra-frame silent periods, respectively.
$\mathbf{\Sigma}_{\mathrm{J}}^{\mathrm{s}}$, $\mathbf{\Sigma}_{\mathrm{J}}^{\mathrm{d}}$, $\mathbf{\Sigma}_{\mathrm{J}}^{\mathrm{i}}$	Covariance matrix of $\mathbf{x}_{\mathrm{J}}^{\mathrm{s}}$, $\mathbf{x}_{\mathrm{J}}^{\mathrm{d}}$, and $\mathbf{x}_{\mathrm{J}}^{\mathrm{i}}$, respectively.
$\mathbf{C}^{\mathrm{s}}$, $\mathbf{C}^{\mathrm{d}}$, $\mathbf{C}^{\mathrm{i}}$	Correlation matrix of $\mathbf{x}_{\mathrm{J}}^{\mathrm{s}}$, $\mathbf{x}_{\mathrm{J}}^{\mathrm{d}}$, and $\mathbf{x}_{\mathrm{J}}^{\mathrm{i}}$, respectively.
$\mathbf{y}_{\mathrm{J}_k}^{\mathrm{s}}$ $\mathbf{y}_{\mathrm{J}_k}^{\mathrm{d}}$ $\mathbf{y}_{\mathrm{J}_k}^{\mathrm{i}}$	Received jamming signals at the kth UE in the (inter-frame) silent, data transmission, and intra-frame silent periods, respectively.
$\mathbf{R}_{\mathrm{J}_k}^{\mathrm{s}}$, $\mathbf{R}_{\mathrm{J}_k}^{\mathrm{d}}$, $\mathbf{R}_{\mathrm{J}_k}^{\mathrm{i}}$	Sample covariance matrix of $\mathbf{y}_{\mathrm{J}_k}^{\mathrm{s}}$, $\mathbf{y}_{\mathrm{J}_k}^{\mathrm{d}}$, and $\mathbf{y}_{\mathrm{J}_k}^{\mathrm{i}}$, respectively.
$\mathbf{Q}_{\mathrm{s}_k}^{\mathrm{s}}$, $\mathbf{Q}_{\mathrm{s}_k}^{\mathrm{d}}$, $\mathbf{Q}_{\mathrm{s}_k}^{\mathrm{i}}$	Matrix whose rows form an orthornomal basis for the left nullspace [25, p. 181] of $\mathbf{y}_{\mathrm{J}_k}^{\mathrm{s}}$, $\mathbf{y}_{\mathrm{J}_k}^{\mathrm{d}}$, and $\mathbf{y}_{\mathrm{J}_k}^{\mathrm{i}}$, respectively.
$\mathbf{Z}_k^{\mathrm{s}}$, $\mathbf{Z}_k^{\mathrm{d}}$, $\mathbf{Z}_k^{\mathrm{i}}$	Jamming channels of the kth UE in the (inter-frame) silent, data transmission, and intra-frame silent periods, respectively.
$\mathbf{Q}_{\mathrm{c}_k}^{\mathrm{s}}$, $\mathbf{Q}_{\mathrm{c}_k}^{\mathrm{d}}$, $\mathbf{Q}_{\mathrm{c}_k}^{\mathrm{i}}$	Matrix whose rows form an orthornomal basis for the left nullspace of $\mathbf{Z}_k^{\mathrm{s}}$, $\mathbf{Z}_k^{\mathrm{d}}$, and $\mathbf{Z}_k^{\mathrm{i}}$, respectively.
$\mathbf{W}_k$	Beam-forming matrix for the kth UE.
$\lvert . \rvert$, $\lvert\lvert . \rvert\rvert$	Complex number's modulus and matrix' Frobenius norm, respectively.
$(.)^T$, $(.)^*$, $(.)^H$, $(.)^{-1}$	Matrix's transpose, conjugate, conjugate (Hermitian) transpose, inverse, respectively.
T_c, T_b, T_ρ	Channel's coherence time, time interval of each frame, and correlation's coherence time, respectively.

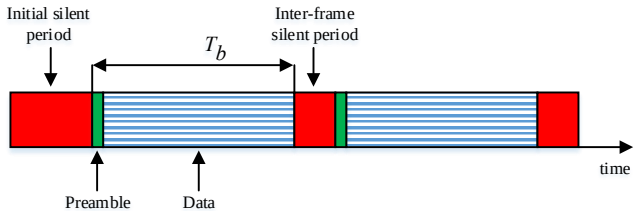

Fig. 2: Baseline protocol.

Based on $\hat{\mathbf{Q}}^{\mathrm{s}}_{\mathrm{s}_k}$, we can design $\mathbf{W}_k$ by selecting B_k rows of $\mathbf{W}_k \in \mathbb{C}^{B_k \times N_k}$ from the $(N_k - N_J)$ rows of $\hat{\mathbf{Q}}^{\mathrm{s}}_{\mathrm{s}_k}$. It is worth noting that B_k should be greater than or equal to D_k for successful BS-UE signal multiplexing at the receiver. Therefore, it is required that $(N_k - N_J) \geq B_k \geq D_k$ for both jamming nullification and BS-UE signal multiplexing. In this paper, we use $\mathbf{W}_k = \hat{\mathbf{Q}}^{\mathrm{s}}_{\mathrm{s}_k}$ (i.e., by setting $B_k = N_k - N_J$), so that the receiver can exploit all of the $(N_k - N_J)$ degree-of-freedoms for signal multiplexing. Because the jamming signals are mostly removed by using $\mathbf{W}_k$, the equivalent channel

$$\mathbf{H}^{\mathrm{eq}}_k = \mathbf{W}_k \mathbf{H}_k \mathbf{P}_k$$

can be estimated by using training signals and a minimum mean-square error (MMSE) or least-square (LS) channel estimator [31]. Equalizers such as MMSE or zero-forcing (ZF) [32, p. 313], can then be applied to find the equalization coefficients, denoted by $\mathbf{G}_k$. Then, BS-UE data transmission can be carried out. Before $\hat{\mathbf{Q}}^{\mathrm{s}}_{\mathrm{s}_k}$ is obsolete, it has to be updated during the inter-frame silent periods. The protocol continues with a $\hat{\mathbf{Q}}^{\mathrm{s}}_{\mathrm{s}_k}$ updating process being carried out after each preamble and data transmission process. A preamble followed by a data transmission period is referred to as a frame. The time interval of each frame is T_b, as illustrated in Fig. 2.

In fact, the effectiveness of the jamming nullification depends on how close $\hat{\mathbf{Q}}^{\mathrm{s}}_{\mathrm{s}_k}$ is to $\mathbf{Q}^{\mathrm{d}}_{\mathrm{s}_k}$, where $\mathbf{Q}^{\mathrm{d}}_{\mathrm{s}_k}$ denotes the matrix whose rows form an orthonormal basis for the left nullspace of the received jamming signals at the kth UE in the data transmission period. The closer $\hat{\mathbf{Q}}^{\mathrm{s}}_{\mathrm{s}_k}$ to $\mathbf{Q}^{\mathrm{d}}_{\mathrm{s}_k}$ results in the better jamming nullification. The first factor that affects the similarity between $\hat{\mathbf{Q}}^{\mathrm{s}}_{\mathrm{s}_k}$ and $\mathbf{Q}^{\mathrm{d}}_{\mathrm{s}_k}$ is how relatively frequently $\hat{\mathbf{Q}}^{\mathrm{s}}_{\mathrm{s}_k}$ is updated. In practice, a more frequent update of $\hat{\mathbf{Q}}^{\mathrm{s}}_{\mathrm{s}_k}$ makes it closer to $\mathbf{Q}^{\mathrm{d}}_{\mathrm{s}_k}$, and certainly leads to less residual jamming after the jamming nullification process. On the other hand, the more frequent update of $\hat{\mathbf{Q}}^{\mathrm{s}}_{\mathrm{s}_k}$ also increases the system's overhead, because the BS-UE channel estimation and synchronization have to be performed at the beginning of each frame. Therefore, less time is available for BS-UE communication. The second factor that affects the similarity between $\hat{\mathbf{Q}}^{\mathrm{s}}_{\mathrm{s}_k}$ and $\mathbf{Q}^{\mathrm{d}}_{\mathrm{s}_k}$, as will be demonstrated in this paper, is how fast the correlations between transmitted jamming signals change. Because of the second factor, the jammers can intentionally vary the correlations to make jamming nullification more challenging.

Given the above relationship between $\hat{\mathbf{Q}}^{\mathrm{s}}_{\mathrm{s}_k}$ and $\mathbf{Q}^{\mathrm{d}}_{\mathrm{s}_k}$. The problems we would like to solve are as follows.

- Characterize the impact of the correlations between transmitted jamming signals on the estimation of $\mathbf{Q}^{\mathrm{s}}_{\mathrm{s}_k}$.
- Characterize the impact of the time-varying correlations on jamming nullification.
- Design jamming nullification techniques for different scenarios of the correlations.

The content of the following sections are as follows. Section III describes the impact of the correlations on the estimation of $\mathbf{Q}^{\mathrm{s}}_{\mathrm{s}_k}$. Then, in Section IV and Section V, we propose jamming nullification techniques for different scenarios of the correlations.

III. Impact of the Correlations between Transmitted Jamming Signals

In this section, we describe the impact of the correlations between transmitted jamming signals on the relationship between $\hat{\mathbf{Q}}^{\mathrm{s}}_{\mathrm{s}_k}$ and $\mathbf{Q}^{\mathrm{d}}_{\mathrm{s}_k}$. Note that, to emphasize the impact of the correlations on the estimation of $\mathbf{Q}^{\mathrm{s}}_{\mathrm{s}_k}$, we assume that the jamming channels are under a slow block fading with coherence time $T_c \gg T_b$. Therefore, the jamming channels are considered unchanged over each frame, such that $\mathbf{Z}^{\mathrm{s}}_k = \mathbf{Z}^{\mathrm{d}}_k = \mathbf{Z}_k$. For brevity, in this section, we only use $\mathbf{Z}_k$ to represent the jamming channels. Correspondingly, we only use $\mathbf{Q}_{\mathrm{c}_k}$ to denote the matrix whose rows form an orthonormal basis of the left nullspace of $\mathbf{Z}_k$, instead of using $\mathbf{Q}^{\mathrm{s}}_{\mathrm{c}_k}$ and $\mathbf{Q}^{\mathrm{d}}_{\mathrm{c}_k}$. We start the section by introducing the algorithm for estimating $\mathbf{Q}^{\mathrm{s}}_{\mathrm{s}_k}$ from the received jamming signals $\mathbf{y}^{\mathrm{s}}_{\mathrm{J}_k}$. We then illustrate the relationship between $\hat{\mathbf{Q}}^{\mathrm{s}}_{\mathrm{s}_k}$ and $\mathbf{Q}^{\mathrm{d}}_{\mathrm{s}_k}$ by comparing them with $\mathbf{Q}_{\mathrm{c}_k}$.

A. Algorithm for Estimating $\mathbf{Q}^{\mathrm{s}}_{\mathrm{s}_k}$

As mentioned in Section II, $\mathbf{Q}^{\mathrm{s}}_{\mathrm{s}_k}$ is estimated in the inter-frame silent periods, during which the BS does not send any signal. Let $\mathbf{y}^{\mathrm{s}}_{\mathrm{J}_k}$ denotes the received jamming signals at the kth UE in the inter-frame silent period, from (1),

$$\mathbf{y}^{\mathrm{s}}_{\mathrm{J}_k} = \mathbf{Z}_k \mathbf{x}^{\mathrm{s}}_{\mathrm{J}} + \mathbf{n}, \tag{5}$$

where $\mathbf{x}^{\mathrm{s}}_{\mathrm{J}}$ is the transmitted jamming signals in the inter-frame silent period. Let

$$\mathbf{R}^{\mathrm{s}}_{\mathrm{J}_k} = \frac{1}{N_{\mathrm{s}}} \mathbf{Y}^{\mathrm{s}}_{\mathrm{J}_k} (\mathbf{Y}^{\mathrm{s}}_{\mathrm{J}_k})^H \tag{6}$$

be a sample covariance matrix of $\mathbf{y}^{\mathrm{s}}_{\mathrm{J}_k}$, where $\mathbf{Y}^{\mathrm{s}}_{\mathrm{J}_k}$ is a sample set containing N_{s} samples of $\mathbf{y}^{\mathrm{s}}_{\mathrm{J}_k}$. We obtain $\hat{\mathbf{Q}}^{\mathrm{s}}_{\mathrm{s}_k}$ by

$$\hat{\mathbf{Q}}^{\mathrm{s}}_{\mathrm{s}_k} = (\mathbf{U}^{\mathrm{s}}_{\mathrm{n}})^H, \tag{7}$$

where $\mathbf{U}^{\mathrm{s}}_{\mathrm{n}} \in \mathbb{C}^{N_k \times (N_k - N_J)}$ is calculated from the singular value decomposition (SVD) of $\mathbf{R}^{\mathrm{s}}_{\mathrm{J}_k}$ [12],

$$\mathbf{R}^{\mathrm{s}}_{\mathrm{J}_k} = [\mathbf{U}^{\mathrm{s}}_{\mathrm{s}}\ \mathbf{U}^{\mathrm{s}}_{\mathrm{n}}] \begin{bmatrix} \mathbf{\Lambda}^{\mathrm{s}}_{\mathrm{s}} & \mathbf{0} \\ \mathbf{0} & \mathbf{\Lambda}^{\mathrm{s}}_{\mathrm{n}} \end{bmatrix} \begin{bmatrix} (\mathbf{U}^{\mathrm{s}}_{\mathrm{s}})^H \\ (\mathbf{U}^{\mathrm{s}}_{\mathrm{n}})^H \end{bmatrix}. \tag{8}$$

Note that, from (6), $\mathbf{R}^{\mathrm{s}}_{\mathrm{J}_k}$ is a Hermitian matrix. Therefore, the SVD shown in (8) is equivalent to an eigen-decomposition (EVD) of $\mathbf{R}^{\mathrm{s}}_{\mathrm{J}_k}$. Consequently, the columns of $\mathbf{U}^{\mathrm{s}}_{\mathrm{s}}$ and $\mathbf{U}^{\mathrm{s}}_{\mathrm{n}}$ are the eigenvectors of $\mathbf{R}^{\mathrm{s}}_{\mathrm{J}_k}$ with the corresponding eigenvalues in the diagonals of $\mathbf{\Lambda}^{\mathrm{s}}_{\mathrm{s}}$ and $\mathbf{\Lambda}^{\mathrm{s}}_{\mathrm{n}}$ in (8), respectively,

$$\begin{aligned} \mathbf{R}^{\mathrm{s}}_{\mathrm{J}_k} \mathbf{u}^{\mathrm{s}}_{\mathrm{n}_i} &= \Lambda^{\mathrm{s}}_{\mathrm{n}_{ii}} \mathbf{u}^{\mathrm{s}}_{\mathrm{n}_i} \\ \mathbf{R}^{\mathrm{s}}_{\mathrm{J}_k} \mathbf{U}^{\mathrm{s}}_{\mathrm{n}} &= \mathbf{\Lambda}^{\mathrm{s}}. \end{aligned} \tag{9}$$

where $\mathbf{u}^{\mathrm{s}}_{\mathrm{n}_i}$ is the ith column of $\mathbf{U}^{\mathrm{s}}_{\mathrm{n}}$, $\Lambda^{\mathrm{s}}_{\mathrm{n}_{ii}}$ is the ith diagonal element of $\mathbf{\Lambda}^{\mathrm{s}}_{\mathrm{n}}$, and $\mathbf{\Lambda}^{\mathrm{s}} \in \mathbb{C}^{N_k \times (N_k - N_J)}$ denotes a matrix with the ith column equal to $\Lambda^{\mathrm{s}}_{\mathrm{n}_{ii}} \mathbf{u}^{\mathrm{s}}_{\mathrm{n}_i}$.

B. Impact of Correlations between Transmitted Jamming Signals

To illustrate the impact of the correlations between transmitted jamming signals on the relationship between $\hat{\mathbf{Q}}^{\mathrm{s}}_{\mathrm{s}_k}$ and $\mathbf{Q}^{\mathrm{d}}_{\mathrm{s}_k}$, we first illustrate the impact of the correlations on the relationship between $\hat{\mathbf{Q}}^{\mathrm{s}}_{\mathrm{s}_k}$ and $\mathbf{Q}_{c_k}$. We do it by analyzing the matrix $\hat{\mathbf{Q}}^{\mathrm{s}}_{\mathrm{s}_k}\mathbf{Z}_k$ in relation to the correlations between transmitted jamming signals.

Theorem 1: $\mathbf{R}^{\mathrm{s}}_{\mathrm{J}_k}$ converges in probability [33, p. 175] to $(\mathbf{Z}_k\mathbf{\Sigma}^{\mathrm{s}}_{\mathrm{J}}\mathbf{Z}^H_k + \sigma^2_n\mathbf{I}_{N_k})$.

Proof: The proof is given in Appendix A. ■

Assuming N_{s} is sufficiently large such that the law of large number is applicable, from (9),

$$
\begin{aligned}
&(\mathbf{Z}_k\mathbf{\Sigma}^{\mathrm{s}}_{\mathrm{J}}\mathbf{Z}^H_k + \sigma^2_n\mathbf{I}_{N_k})\mathbf{U}^{\mathrm{s}}_{\mathrm{n}} = \mathbf{\Lambda}^{\mathrm{s}}\\
&\mathbf{Z}_k\mathbf{\Sigma}^{\mathrm{s}}_{\mathrm{J}}\mathbf{Z}^H_k\mathbf{U}^{\mathrm{s}}_{\mathrm{n}} = \mathbf{\Lambda}^{\mathrm{s}} - \sigma^2_n\mathbf{U}^{\mathrm{s}}_{\mathrm{n}}\\
&\hat{\mathbf{Q}}^{\mathrm{s}}_{\mathrm{s}_k}\mathbf{Z}_k\mathbf{\Sigma}^{\mathrm{s}}_{\mathrm{J}}\mathbf{Z}^H_k = (\mathbf{\Lambda}^{\mathrm{s}} - \sigma^2_n\mathbf{U}^{\mathrm{s}}_{\mathrm{n}})^H\\
&\hat{\mathbf{Q}}^{\mathrm{s}}_{\mathrm{s}_k}\mathbf{Z}_k = \frac{(\mathbf{\Sigma}^{\mathrm{s}}_{\mathrm{Jf}})^T}{\det(\mathbf{\Sigma}^{\mathrm{s}}_{\mathrm{J}})}(\mathbf{\Lambda}^{\mathrm{s}} - \sigma^2_n\mathbf{U}^{\mathrm{s}}_{\mathrm{n}})^H\mathbf{Z}_k(\mathbf{Z}^H_k\mathbf{Z}_k)^{-1}, \qquad (10)
\end{aligned}
$$

where $\mathbf{\Sigma}^{\mathrm{s}}_{\mathrm{Jf}}$ denotes the cofactor matrix [25, p. 275] of $\mathbf{\Sigma}^{\mathrm{s}}_{\mathrm{J}}$. The matrix $\mathbf{\Sigma}^{\mathrm{s}}_{\mathrm{J}}$ can be expressed by the variances of the transmitted jamming signals and the correlations between them,

$$
\mathbf{\Sigma}^{\mathrm{s}}_{\mathrm{J}} = \begin{bmatrix} \sigma^2_1 & \rho^{\mathrm{s}}_{12}\sigma_1\sigma_2 & \dots & \rho^{\mathrm{s}}_{1N_J}\sigma_1\sigma_{N_J} \\ (\rho^{\mathrm{s}}_{12})^*\sigma_1\sigma_2 & \sigma^2_2 & \dots & \rho^{\mathrm{s}}_{2N_J}\sigma_2\sigma_{N_J} \\ \dots & \dots & \dots & \dots \\ (\rho^{\mathrm{s}}_{1N_J})^*\sigma_1\sigma_{N_J} & (\rho^{\mathrm{s}}_{2N_J})^*\sigma_2\sigma_{N_J} & \dots & \sigma^2_{N_J} \end{bmatrix}, \qquad (11)
$$

where σ^2_j is the variance of the jth transmitted jamming signal, and ρ^{s}_{ij} is the complex correlation coefficient between the ith and jth transmitted jamming signals in the inter-frame silent period, with $i, j \in \{1, 2, ...N_J\}$. The complex correlation coefficient ρ^{s}_{ij} can be calculated as [34, p. 87]

$$
\rho^{\mathrm{s}}_{ij} = \frac{\mathbb{E}(\mathbf{X}^{\mathrm{s}}_{\mathrm{J}i}(\mathbf{X}^{\mathrm{s}}_{\mathrm{J}j})^H)}{\sigma_i\sigma_j}. \qquad (12)
$$

The correlation matrix [33, p. 139] of the transmitted jamming signals can be expressed as

$$
\mathbf{C}^{\mathrm{s}} = \begin{bmatrix} 1 & \rho^{\mathrm{s}}_{12} & \dots & \rho^{\mathrm{s}}_{1N_J} \\ (\rho^{\mathrm{s}}_{12})^* & 1 & \dots & \rho^{\mathrm{s}}_{2N_J} \\ \dots & \dots & \dots & \dots \\ (\rho^{\mathrm{s}}_{1N_J})^* & (\rho^{\mathrm{s}}_{2N_J})^* & \dots & 1 \end{bmatrix} \qquad (13)
$$

and can be calculated from $\mathbf{\Sigma}^{\mathrm{s}}_{\mathrm{J}}$ by

$$
\mathbf{C}^{\mathrm{s}} = \mathbf{D}^{-1}\mathbf{\Sigma}^{\mathrm{s}}_{\mathrm{J}}\mathbf{D}^{-1}, \qquad (14)
$$

where $\mathbf{D}$ is a $N_J \times N_J$ diagonal matrix with the jth diagonal element being σ_j, and is referred to as the standard deviation matrix of the transmitted jamming signals.

Observation on the elements of $\hat{\mathbf{Q}}^{\mathrm{s}}_{\mathrm{s}_k}\mathbf{Z}_k$*:* from (10), we can see that the elements of $\hat{\mathbf{Q}}^{\mathrm{s}}_{\mathrm{s}_k}\mathbf{Z}_k$ approach infinity when $|\rho^{\mathrm{s}}_{ij}| \to 1$, where $|.|$ denotes the modulus of a complex number. It is because when $|\rho^{\mathrm{s}}_{ij}| \to 1$, the correlation matrix $\mathbf{C}^{\mathrm{s}}$ becomes singular. Therefore, from (14), $\mathbf{\Sigma}^{\mathrm{s}}_{\mathrm{J}}$ becomes a singular matrix. As a result, $\det(\mathbf{\Sigma}^{\mathrm{s}}_{\mathrm{J}}) \to 0$. This makes the elements of $\hat{\mathbf{Q}}^{\mathrm{s}}_{\mathrm{s}_k}\mathbf{Z}_k$ approach infinity.

This observation is demonstrated in Fig. 3 which shows the normalized residual value, $r_{\mathrm{c}} = ||\hat{\mathbf{Q}}^{\mathrm{s}}_{\mathrm{s}_k}\mathbf{Z}_k||^2/||\mathbf{Z}_k||^2$, as a function of $|\rho^{\mathrm{s}}_{12}|$ using different distribution functions for the transmitted jamming signals, including the Gaussian, uniform, and Chi-square (with 2 degrees-of-freedom) distribution functions. The number of jammer is $N_J = 2$, the UE antennas is $N_k = 8$, and $||.||$ denotes matrix's Frobenius norm. As can be seen, without noise, $r_{\mathrm{c}} = 0$ for any value of $|\rho^{\mathrm{s}}_{12}|$ except for $|\rho^{\mathrm{s}}_{12}| = 1$. It is because when $\sigma^2_n = 0$, all the diagonal elements of $\mathbf{\Lambda}^{\mathrm{s}}_{\mathrm{n}}$ are zero, and (10) becomes

$$
\hat{\mathbf{Q}}^{\mathrm{s}}_{\mathrm{s}_k}\mathbf{Z}_k = \frac{(\mathbf{\Sigma}^{\mathrm{s}}_{\mathrm{Jf}})^T}{\det(\mathbf{\Sigma}^{\mathrm{s}}_{\mathrm{J}})}\mathbf{0}_{(N_k-N_J,N_k)}\mathbf{Z}_k(\mathbf{Z}^H_k\mathbf{Z}_k)^{-1},
$$

where $\mathbf{0}_{(N_k-N_J,N_k)} \in \mathbb{C}^{(N_k-N_J)\times N_k}$ denotes a null matrix. On the other hand, in the presence of noise with a received signal to noise ratio (SNR) of 14 dB, r_{c} is small and stable for small values of $|\rho^{\mathrm{s}}_{12}|$. However, r_{c} increases dramatically when $|\rho^{\mathrm{s}}_{12}|$ approaches 1, meaning the transmitted jamming signals are highly correlated.

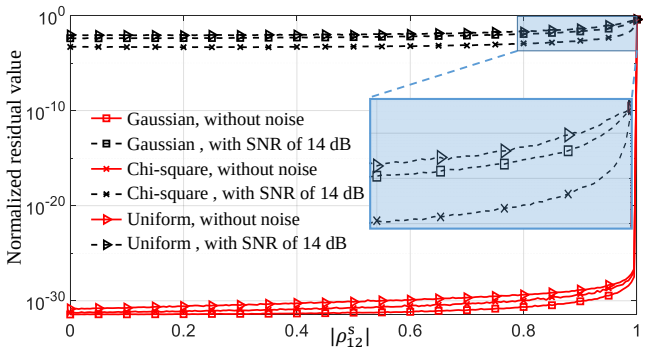

Fig. 3: r_{c} values for different $|\rho^{\mathrm{s}}_{12}|$.

Therefore, when the jamming signals are uncorrelated, the elements of $\hat{\mathbf{Q}}^{\mathrm{s}}_{\mathrm{s}_k}\mathbf{Z}_k$ are small, meaning $\hat{\mathbf{Q}}^{\mathrm{s}}_{\mathrm{s}_k}$ is close to $\mathbf{Q}_{\mathrm{c}_k}$. Similarly, $\mathbf{Q}^{\mathrm{d}}_{\mathrm{s}_k}$ is close to $\mathbf{Q}_{\mathrm{c}_k}$ when the jamming signals are uncorrelated. Therefore, $\hat{\mathbf{Q}}^{\mathrm{s}}_{\mathrm{s}_k}$ is close to $\mathbf{Q}^{\mathrm{d}}_{\mathrm{s}_k}$ and can be used to nullify $\mathbf{y}^{\mathrm{d}}_{\mathrm{J}_k}$. However, when the correlations between transmitted jamming signals are large, there are large values in the elements of $\hat{\mathbf{Q}}^{\mathrm{s}}_{\mathrm{s}_k}\mathbf{Z}_k$, meaning $\hat{\mathbf{Q}}^{\mathrm{s}}_{\mathrm{s}_k}$ is not close to $\mathbf{Q}_{\mathrm{c}_k}$. Therefore, $\hat{\mathbf{Q}}^{\mathrm{s}}_{\mathrm{s}_k}$ may not be close to $\mathbf{Q}^{\mathrm{d}}_{\mathrm{s}_k}$ and using $\mathbf{W}_k$ derived from $\hat{\mathbf{Q}}^{\mathrm{s}}_{\mathrm{s}_k}$ may not guarantee jamming nullification.

Accordingly, we need different techniques to suppress the jamming signals for different correlations between transmitted jamming signals. In the next section, we consider the case of uncorrelated jamming signals (i.e., the correlations are zero), which is the assumption in most existing studies [12]–[16]. Then, in Section V, we consider different scenarios of non-zero correlations.

IV. Jamming Nullification with Uncorrelated Transmitted Jamming Signals and Time-varying Channels

This section describes jamming nullification when the jamming signals are uncorrelated, which is an assumption in most of the existing jamming suppression techniques [12]–[16]. The technique in this section is developed to deal with time-varying channels.

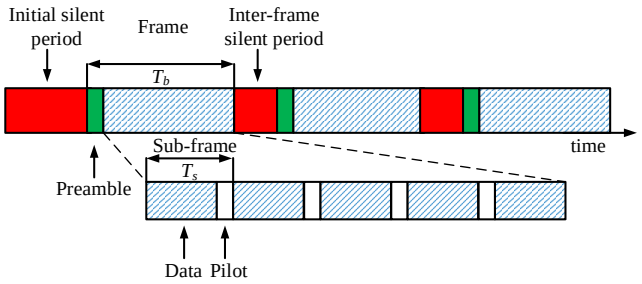

Fig. 4: Protocol for time-varying channels.

Algorithm 1 Protocol for time-varying channels.

1: Acquire $\hat{\mathbf{Q}}^{\mathrm{s}}_{\mathrm{s}_k}$ during the initial silent period or update $\hat{\mathbf{Q}}^{\mathrm{s}}_{\mathrm{s}_k}$ during inter-frame silent periods.
2: Design $\mathbf{W}_k$ from $\hat{\mathbf{Q}}^{\mathrm{s}}_{\mathrm{s}_k}$.
3: Estimate $\mathbf{H}^{\mathrm{eq}}_k$ using the preamble.
4: Calculate equalization coefficients $\mathbf{G}_k$.
5: Perform BS-UE data transmission.
6: $n_{\mathrm{sf}} \leftarrow 1$
7: **while** $n_{\mathrm{sf}} \leq N_{\mathrm{sf}} - 1$ **do**
8: Update $\mathbf{G}_k$ using $\mathbf{x}_{\mathrm{m}_k}$.
9: Perform BS-UE data transmission.
10: $n_{\mathrm{sf}} \leftarrow n_{\mathrm{sf}} + 1$
11: **end while**
12: Repeat from 1.

A. Protocol for Time-varying Channels

We revise the baseline protocol in Fig. 2 to that in Fig. 4 and Alg. 1 to deal with time-varying BS-UE and jamming channels. Similar to the protocol in Fig. 2, the protocol in Fig. 4 also consists of an initial silent period for the acquisition of $\hat{\mathbf{Q}}^{\mathrm{s}}_{\mathrm{s}_k}$, and inter-frame silent periods between frames to update $\hat{\mathbf{Q}}^{\mathrm{s}}_{\mathrm{s}_k}$. Each frame starts by a preamble which contains a short training sequence (STS) and a long training sequence (LTS). The STS is used for frame detection and fine timing, and carrier frequency offset (CFO) estimation. The LTS is used for BS-UE channel estimation. However, different from the baseline protocol in Fig. 2, each frame in Fig. 4 is divided into N_{sf} sub-frames, each of length $T_s = T_b/N_{\mathrm{sf}}$. Each sub-frame consists of data payload and pilot samples $\mathbf{x}_{\mathrm{m}_k}$, which is used for updating equalization coefficients $\mathbf{G}_k$ by the adaptive equalizer described below.

B. Adaptive Equalization

To deal with time-varying UE channels, we propose to use one of several optional adaptive equalizers, whose equalization coefficients can be adapted to channel variations. There have been a few types of adaptive filters being reported in the literature, such as the modified complex gradient-projection-II (MCG-P-II) [35] and the adaptive decision feedback equalizer (DFE) for V-BLAST systems [36]. Based on the DFE, we also develop an adaptive equalizer with the recursive least square (RLS) principle, without using decision/pilot based feedback. This is realized by removing the feed-backward filter but only keeping the feed-forward filter in the DFE as described in [36]. We call it RLS-FFE. Compared to DFE, the RLS-FFE has lower computational complexity, and is shown to work well using simulation.

In summary, when the transmitted jamming signals are uncorrelated, we use the communication protocol represented in Fig. 4 and Algorithm 1 to nullify the jamming signals and perform BS-UE data transmission. In the next section, we consider the case with non-zero correlations between transmitted jamming signals.

V. Jamming Nullification with Correlated Transmitted Jamming Signals

In this section, we investigate jamming nullification when the transmitted jamming signals are correlated. Similar to Section III, to emphasize the impact of the correlations, we assume that the jamming channels are unchanged over each frame, and use $\mathbf{Z}_k$ only to denote the jamming channels. First, we demonstrate that the change in the correlations between transmitted jamming signals causes a "virtual change" in the jamming channels. Therefore, even though $\mathbf{Z}_k$ is unchanged, using $\mathbf{W}_k$ deriving from $\hat{\mathbf{Q}}^{\mathrm{s}}_{\mathrm{s}_k}$ may not guarantee jamming nullification performance. Then, we analyze jamming nullification for two schemes of non-zero correlations between transmitted jamming signals.

Theorem 2: Let

$$\mathbf{\Sigma}^{\mathrm{s}}_{\mathrm{J}} = \mathbf{V}^{\mathrm{s}}\mathbf{S}^{\mathrm{s}}(\mathbf{V}^{\mathrm{s}})^H \text{ and } \mathbf{\Sigma}^{\mathrm{d}}_{\mathrm{J}} = \mathbf{V}^{\mathrm{d}}\mathbf{S}^{\mathrm{d}}(\mathbf{V}^{\mathrm{d}})^H$$

be the SVD of $\mathbf{\Sigma}^{\mathrm{s}}_{\mathrm{J}}$ and $\mathbf{\Sigma}^{\mathrm{d}}_{\mathrm{J}}$, respectively. Let $\mathbf{F}$ be the "virtual change" factor given by

$$\mathbf{F} = \mathbf{V}^{\mathrm{d}}\sqrt{\mathbf{S}^{\mathrm{d}}(\mathbf{S}^{\mathrm{s}})^{-1}}(\mathbf{V}^{\mathrm{s}})^H. \tag{15}$$

Then, the change over time from $\mathbf{\Sigma}^{\mathrm{s}}_{\mathrm{J}}$ to $\mathbf{\Sigma}^{\mathrm{d}}_{\mathrm{J}}$ causes a "virtual change" in the jamming channels from $\mathbf{Z}_k$ to $(\mathbf{Z}_k\mathbf{F})$.

Proof: The proof is given in Appendix B. ■

Examining the behavior of $\mathbf{F}$ provides us interesting insights about the impact of the change in the correlations between transmitted jamming signals on the "virtual change" in the jamming channels. The first observation is for the case of unchanged (i.e., over each frame) correlations, such that $\mathbf{C}^{\mathrm{d}} = \mathbf{C}^{\mathrm{s}}$. In this case, $\mathbf{\Sigma}^{\mathrm{d}}_{\mathrm{J}} = \mathbf{\Sigma}^{\mathrm{s}}_{\mathrm{J}}$, $\mathbf{V}^{\mathrm{d}} = \mathbf{V}^{\mathrm{s}}, \mathbf{S}^{\mathrm{d}} = \mathbf{S}^{\mathrm{s}}$, and $\mathbf{F} = \mathbf{I}$. Therefore, $\mathbf{Z}_k\mathbf{F} = \mathbf{Z}_k$, and there is no "virtual change" in the jamming channels. The case of unchanged correlations between transmitted jamming signals will be considered in more detail in Subsection V-A. The second observation is for the case of time-varying correlations, and is described by the following corollary.

Corollary 2.1*:* When $\mathbf{C}^{\mathrm{d}} \neq \mathbf{C}^{\mathrm{s}}$ and $|\rho^{\mathrm{s}}_{ij}| \rightarrow 1$ for $i \neq j$, the elements of the "virtual change" factor $\mathbf{F}$ approach infinity, results in a significant "virtual change" in the jamming channels.

Proof: when $|\rho^{\mathrm{s}}_{ij}| \rightarrow 1$, $\mathbf{C}^{\mathrm{s}}$ becomes a singular matrix. From (14), $\mathbf{\Sigma}^{\mathrm{s}}_{\mathrm{J}}$ is also a singular matrix. Therefore, there is one diagonal element $s^{\mathrm{s}}_{jj} \in \mathbf{S}^{\mathrm{s}}$ approaches 0 [37, p. 261]. From (15), when $s^{\mathrm{s}}_{jj} \in \mathbf{S}^{\mathrm{s}}$ approach 0 while $s^{\mathrm{d}}_{jj} \in \mathbf{S}^{\mathrm{d}}$ is not equal to s^{s}_{jj}, the elements of $\mathbf{F}$ approach infinity. ■

Therefore, there is a "virtual change" in the jamming channels observed by the receiver when the correlations

between transmitted jamming signals vary over time. The "virtual change" is significant when $|\rho_{ij}^{\mathrm{s}}| \to 1$ for $i \neq j$. It implies that, from the receiver's observation, the estimated left nullspace becomes ineffective when the correlation is high and largely changed. Therefore, using $\hat{\mathbf{Q}}_{\mathrm{s}_k}^{\mathrm{s}}$ to generate $\mathbf{W}_k$ may not guarantee jamming nullification in the data transmission period. The case of time-varying correlations between transmitted jamming signals will be considered in more detail in Subsection V-B.

A. Jamming Nullification with Unchanged Non-zero Correlations

In this subsection, we consider the case of $T_\rho \geq T_b$, where T_ρ denotes the correlation coherence time, over which the change in the correlations is negligible, and T_b is the time interval of one frame as illustrated in Fig. 4. During the inter-frame silent period and data transmission period, $\mathbf{C}^{\mathrm{d}} = \mathbf{C}^{\mathrm{s}}$.

As described in the first observation on the behavior of $\mathbf{F}$, when $\mathbf{C}^{\mathrm{d}} = \mathbf{C}^{\mathrm{s}}$, we have $\mathbf{\Sigma}_{\mathrm{J}}^{\mathrm{d}} = \mathbf{\Sigma}_{\mathrm{J}}^{\mathrm{s}}$, $\mathbf{V}^{\mathrm{d}} = \mathbf{V}^{\mathrm{s}}, \mathbf{S}^{\mathrm{d}} = \mathbf{S}^{\mathrm{s}}$, and $\mathbf{F} = \mathbf{I}$. Therefore, there is no "virtual change" in the jamming channels. As a result, the beam-forming matrix $\mathbf{W}_k$, which is derived from $\hat{\mathbf{Q}}_{\mathrm{s}_k}^{\mathrm{s}}$, can be used to nullify $\mathbf{y}_{\mathrm{J}_k}^{\mathrm{d}}$, regardless of the value of the correlations between transmitted jamming signals.

Therefore, jamming signals with non-zero and unchanged correlations can be suppressed in the same manner as the uncorrelated jamming signals in Section IV. In these cases, we only have to handle the time-varying channels, but not the time-varying correlations between transmitted jamming signals. Hence, the protocol in Fig. 4 and Algorithm 1 can be used to nullify the jamming signals and perform BS-UE communication. In the following sub-section, we investigate the case of time-varying non-zero correlations.

B. Jamming Nullification with Time-varying Non-zero Correlations

In this sub-section, we consider the case of $T_\rho < T_b$, meaning the correlations between transmitted jamming signals vary rapidly enough, such that during the frame interval T_b, the change in the correlations is not negligible. As stated in Theorem 2, the change in the correlations causes a "virtual change" in the jamming channels, characterized by the "virtual change" factor

$$\mathbf{F} = \mathbf{V}^{\mathrm{d}} \sqrt{\mathbf{S}^{\mathrm{d}} (\mathbf{S}^{\mathrm{s}})^{-1}} (\mathbf{V}^{\mathrm{s}})^{H}.$$

Moreover, from Corollary 2.1, when $\mathbf{C}^{\mathrm{d}} \neq \mathbf{C}^{\mathrm{s}}$ and the absolute value of one or more off-diagonal element of $\mathbf{C}^{\mathrm{s}}$ approach 1, there is a significant "virtual change" in the jamming channels. The significant "virtual change" in the jamming channels (now $\mathbf{Z}_k\mathbf{F}$) make it unable to use $\mathbf{W}_k$, which derived from $\hat{\mathbf{Q}}_{\mathrm{s}_k}^{\mathrm{s}}$, to nullify the jamming signals in data transmission period $\mathbf{y}_{\mathrm{J}_k}^{\mathrm{d}}$.

A potential solution to the change in the correlations is to decrease the frame time interval to $T_b \leq T_\rho$. However, more frequent tracking of $\hat{\mathbf{Q}}_{\mathrm{s}_k}^{\mathrm{s}}$ means less BS-UE data transmission time. A suitable value of T_b should be based on two factors: the jamming channels' coherence time T_c and the correlation coherence time T_ρ. For example, the longer T_c or the longer T_ρ, the longer T_b should be. While the first factor depends on the nature of the jamming channels environment, and its value can be predicted based on field measurement, we cannot control or predict the second factor.

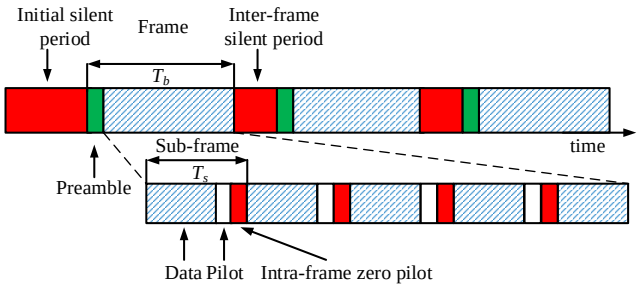

Fig. 5: Protocol for time-varying correlations and time-varying channels.

Algorithm 2 Protocol for time-varying correlations and time-varying channels.

1: Acquire $\hat{\mathbf{Q}}_{\mathrm{s}_k}^{\mathrm{s}}$ during the initial silent period or update $\hat{\mathbf{Q}}_{\mathrm{s}_k}^{\mathrm{s}}$ during inter-frame silent periods.
2: Design $\mathbf{W}_k$ from $\hat{\mathbf{Q}}_{\mathrm{s}_k}^{\mathrm{s}}$.
3: Estimate $\mathbf{H}_k^{\mathrm{eq}}$ using the preamble.
4: Calculate equalization coefficients $\mathbf{G}_k$.
5: Perform BS-UE data transmission.
6: $n_{\mathrm{sf}} \leftarrow 1$
7: **while** $n_{\mathrm{sf}} \leq N_{\mathrm{sf}} - 1$ **do**
8: Update $\mathbf{G}_k$ using $\mathbf{x}_{\mathrm{m}_k}$.
9: Measure $\gamma_{\mathrm{J}} = ||\mathbf{r}_k||^2 / ||\mathbf{p}_k||^2$ using $\mathbf{x}_{\mathrm{m}_k}$.
10: **if** $\gamma_{\mathrm{J}} \geq \gamma_{\mathrm{r}}$ **then**
11: Start intra-frame zero pilot.
12: Estimate $\mathbf{Q}_{\mathrm{s}_k}^{\mathrm{i}}$ during intra-frame zero pilot.
13: Design $\mathbf{W}_k^{\mathrm{i}}$ from $\hat{\mathbf{Q}}_{\mathrm{s}_k}^{\mathrm{i}}$.
14: Update equivalent channel $\mathbf{H}_k^{\mathrm{eq}} \leftarrow \mathbf{W}_k^{\mathrm{i}} \mathbf{W}_k^{H} \mathbf{H}_k^{\mathrm{eq}}$.
15: Update beam-forming matrix $\mathbf{W}_k \leftarrow \mathbf{W}_k^{\mathrm{i}}$.
16: **end if**
17: Perform BS-UE data transmission.
18: $n_{\mathrm{sf}} \leftarrow n_{\mathrm{sf}} + 1$
19: **end while**
20: Repeat from 1.

Given the above, we develop a communication protocol capable of dealing with the change of the correlations between transmitted jamming signals, as shown in Fig. 5 and Algorithm 2. This protocol has two differences compared to that in Fig. 4 and Alg. 1. First, the pilot signal $\mathbf{x}_{\mathrm{m}_k}$, demonstrated by white color in Fig. 5, in addition to the first use to update equalization coefficient $\mathbf{G}_k$, is also used to measure the jamming residual. Second, when the measured jamming residual is higher than a predefined value, intra-frame zero pilot is used to update the beam-forming matrix $\mathbf{W}_k$, as described below. By using the pilot signal $\mathbf{x}_{\mathrm{m}_k}$, the jamming

residual can be measured by

$$\mathbf{r}_k = \mathbf{p}_k - \mathbf{W}_k(\mathbf{H}_k\mathbf{P}_k\mathbf{x}_{\mathrm{m}_k} + \mathbf{H}_k\sum_{l\neq k}^{K}\mathbf{P}_l\mathbf{x}_l) = \mathbf{W}_k(\mathbf{Z}_k\mathbf{x}_{\mathrm{J}} + \mathbf{n}).$$

When the normalized residual value $\gamma_{\mathrm{J}} = ||\mathbf{r}_k||^2/||\mathbf{p}_k||^2$ exceeds a pre-defined threshold γ_{r}, the BS starts sending intra-frame zero pilots, and $\mathbf{Q}^{\mathrm{i}}_{\mathrm{s}_k}$ is estimated using the SVD as described in Section III. As shown in Table I, $\mathbf{Q}^{\mathrm{i}}_{\mathrm{s}_k}$ denotes a matrix whose rows form an orthornomal basis for the left nullspace of the received signal at the kth UE in the intra-frame silent period. The new beam-forming matrix $\mathbf{W}^{\mathrm{i}}_k$ is obtained from $\hat{\mathbf{Q}}^{\mathrm{i}}_{\mathrm{s}_k}$, which is the estimated value of $\mathbf{Q}^{\mathrm{i}}_{\mathrm{s}_k}$. Note that a smaller value of γ_{r} results in better jamming nullification, and therefore less error in the BS-UE data transmission. However, reducing the normalized residual threshold also results in more intra-frame zero pilot activation, and less time for BS-UE communication. Note also that starting the intra-frame zero pilots only reduces the spectral efficiency of the UEs that do not request it. However, the communication between the UE that needs intra-frame zero pilots and the BS will be completely lost if the intra-frame zero pilots is not activated. Therefore, the BS starts the intra-frame zero pilots whenever requested from one or more UE.

To reduce the system's overhead, the equivalent channel is only estimated using training signal and an MMSE or LS estimator once per frame. For each sub-frame, when intra-frame zero pilot is used, $\mathbf{H}^{\mathrm{eq}}_k$ is replaced by $\mathbf{H}^{\mathrm{eq\_i}}_k$ given by

$$\mathbf{H}^{\mathrm{eq\_i}}_k = \mathbf{W}^{\mathrm{i}}_k\mathbf{H}_k\mathbf{P}_k = \mathbf{W}^{\mathrm{i}}_k\mathbf{W}^{H}_k\mathbf{W}_k\mathbf{H}_k\mathbf{P}_k = \mathbf{W}^{\mathrm{i}}_k\mathbf{W}^{H}_k\mathbf{H}^{\mathrm{eq}}_k.$$

By using the pilots signal $\mathbf{x}_{\mathrm{m}_k}$ and intra-frame zero pilots, we divide each frame with a time interval T_b into N_{sf} sub-frames with a time interval T_s. This division significantly reduces the change in the correlations between transmitted jamming signals and reduces the elements of the "virtual change" factor $\mathbf{F}$. Therefore, jamming nullification performance can be significantly improved.

It is worth noting that we can start an inter-frame silent period as soon as γ_{J} exceeds γ_{r}. However, starting a new inter-frame silent period requires the BS-UE synchronization and $\mathbf{H}^{\mathrm{eq}}_k$ estimation to be performed again. Therefore, valuable BS-UE communication time is reduced dramatically when T_ρ decreases. Therefore, using the intra-frame zero pilot as in Fig. 5 and Algorithm 2 to combat the change in the correlations between transmitted jamming signals is a more suitable approach to reduce the overhead of the system and increase BS-UE communication time.

VI. Simulation Result

This section presents the simulation results to validate our proposed schemes. The performance metrics include the normalized residual value $r_{\mathrm{J}} = \frac{||\hat{\mathbf{Q}}^{\mathrm{s}}_{\mathrm{s}_k}\mathbf{y}^{\mathrm{d}}_{\mathrm{J}_k}||^2}{||\mathbf{y}^{\mathrm{d}}_{\mathrm{J}_k}||^2}$ and the bit error rate (BER). The simulation parameters are as follows unless otherwise stated. A single carrier narrowband MIMO system is considered with a bandwidth of 200 kHz and a center frequency of 447 MHz. The symbol duration is 5 μs. Note that as reported in [38], the typical root mean square (RMS) delay spread value in an urban area is 0.73 μs, corresponding to a coherence bandwidth of about 685 kHz [39, p. 45]. The RMS delay spreads in the suburban and combined areas are smaller than that in the urban area, corresponding to larger coherence bandwidths. We use 16 Quadrature Amplitude Modulation (QAM) with no forward error correction (FEC) coding. Both BS-UE and jammers-UE channels are modeled using a flat fast fading Rician model from [28] with a Doppler frequency of $F_d = 24.83$ Hz (i.e., corresponding to BS-UE and jammers-UE relative speeds of about 60 km/h), and a Rician factor of 5. The number of propagation paths for each signal is 5. The path losses over BS-UE channel and jammer-UE channel are both modeled using the COST 231 Hata model [27, p. 135] with $h_{\mathrm{BS}} = h_{\mathrm{J}} = 50$m, $h_{\mathrm{UE}} = 10$m, and $d_{\mathrm{BS}} = d_{\mathrm{J}} = 1$km, where h_{BS}, h_{J}, h_{UE}, d_{BS}, and d_{J} denote the BS height, jammer height, UE height, BS-UE distance, and the distance from each jammer to the UE, respectively. The ratio of transmitted jamming power to BS transmitted power is 3. The BS and UE have a uniform linear array (ULA) with 12 and 8 antennas, respectively. The BS is communicating with $K = 4$ UEs. The number of samples in the initial silent periods, inter-frame zero pilots, intra-frame zero pilots, and $\mathbf{x}_{\mathrm{m}_k}$ are 64, 5, 5 and 5, respectively. Note that in order to obtain a fair comparison about the efficiency of the adaptive equalizer and the beam-forming matrix in jamming nullification, we used the same number of samples for inter-frame zero pilot, intra-frame zero pilot, and $\mathbf{x}_{\mathrm{m}_k}$. All the simulation results are obtained by averaging over 500 independent trials.

A. Uncorrelated Jamming Signals

In this sub-section, we provide simulation results for the case of uncorrelated transmitted jamming signals. As demonstrated in Section IV, we use the inter-frame silent period to update the beam-forming matrix and one of four equalizers (i.e., ZF, MCG-P-II, DFE, and RLS-FFE equalizers) to update the equalizer coefficient $\mathbf{G}_k$. To demonstrate the effectiveness in suppressing the jamming signals of the beam-forming matrix and the adaptive equalizer, we simulate the system using the following scenarios:

- *No jammer*: There is no jammer in the system;
- *Ideal*: Beam-forming matrix is derived directly from the known jamming channels;
- *Inter-frame*: Beam-forming matrix is acquired during the initial silent period and updated using inter-frame zero pilots;
- *Initial*: Beam-forming matrix is acquired during the initial silent period, without updating.

Table II shows the performance of different equalizers for different beam-forming matrix updating scenarios. The SNR used for simulation is 25 dB. As can be seen, in the presence of jammers, the adaptive equalizers (i.e., MCG-P-II, RLS-FFE, and DFE) all achieve better performance than the ZF equalizer for all of the beam-forming matrix updating scenarios. Moreover, the adaptive equalizers using the *initial* beam-forming matrix updating scenario achieve a higher BER compared to that of the ZF equalizer using the *inter-frame* beam-forming matrix updating scenario. It means the beam-forming matrix is more efficient than the adaptive equalizer in dealing with the jamming signals. It is because varied jamming

TABLE II: BER performance for various equalizers.

Scenarios	ZF	MCG-P-II	RLS-FFE	DFE
No jammer	0.0026	0.0028	0.0029	0.0021
Ideal	0.0230	0.0234	0.0256	0.0286
Inter-frame	0.0610	0.0586	0.0499	0.0497
Initial	0.3168	0.1074	0.0811	0.0834

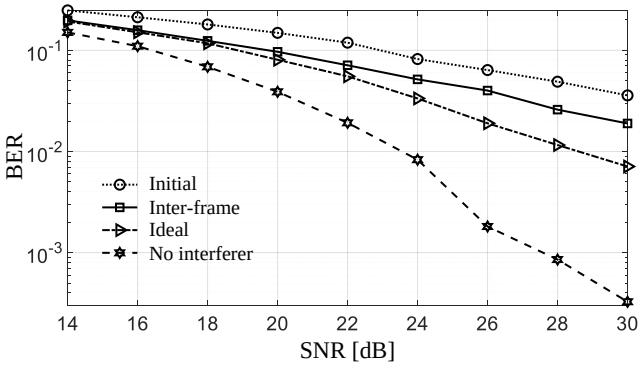

Fig. 6: BER performance of MCG-P-II.

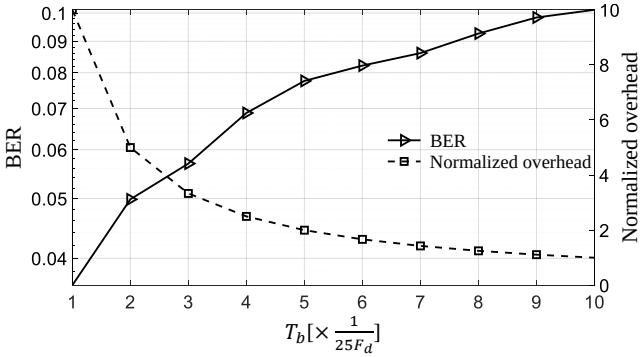

Fig. 7: BER and overhead trade-off for different values of T_b.

nullspace mainly causes increased jamming, similar to noise, while adaptive equalizers are developed based on structured signal models. Among the adaptive equalizers, MCG-P-II achieves only slightly higher BER compared to the other ones. On the other hand, while MCG-P-II has a computational complexity of $\mathcal{O}((N_k - N_J)^2)$ [35], both DFE and RLS-FFE have $\mathcal{O}((N_k - N_J)^3)$ [36]. Therefore, MCG-P-II achieves a better balance between performance and complexity, and is regarded as the best option. Accordingly, from Fig. 6 onwards, we use MCG-P-II to generate simulation results.

Fig. 6 illustrates MCG-P-II's BER performance with different beam-forming matrix updating scenarios and different SNR values. As can be seen, the *inter-frame* beam-forming matrix updating scenario can successfully nullify the jamming signals, results in system performance of only about 3 dB performance degradation compared to that of the system with *ideal* knowledge about the jamming channels.

Fig. 7 illustrates the BER performance and the normalized overhead of the system as functions of T_b, which quantifies how frequent the beam-forming matrix is updated. For comparison purposes, the overhead is normalized such that the normalized overhead when $T_b = \frac{1}{25F_d}$ is 1. As can be seen, there is a trade-off between the BER and the overhead of the system. When T_b increases, the BER of the system increases, whereas the overhead of the system decrease, and vice versa.

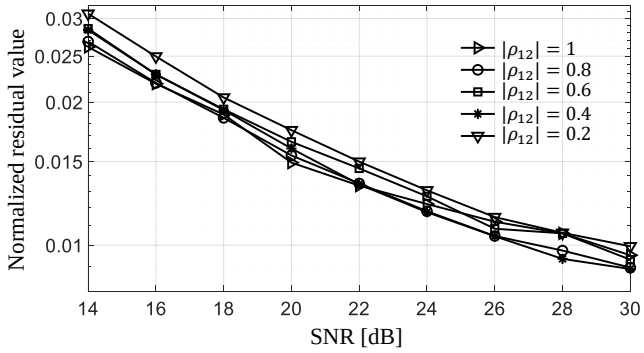

Fig. 8: r_{J} values when $|\rho_{12}|$ is unchanged.

B. Unchanged Non-Zero Correlations

In this sub-section, we present the simulation results for the case of non-zero correlations between transmitted jamming signals, and with $T_\rho \geq T_b$, such that the correlations are considered constant over each frame. As discussed in Subsection V-A, when the correlations between the transmitted jamming signals are non-zero and constant, there is no "virtual change" in the jamming channels. As a result, we only have to deal with time-varying physical channels. Therefore, the protocol in Fig. 4 and Alg. 1 can be used to nullify jamming signals and perform BS-UE communication.

Fig. 8 illustrates the values of r_{J} as a function of the jamming signals' SNR for different values of $\rho_{12}^{\mathrm{s}} = \rho_{12}^{\mathrm{d}} = \rho_{12}$. As can be seen, r_{J} has similar values for different $|\rho_{12}|$ values, meaning the value of $|\rho_{12}|$ have a little impact on the jamming nullification performance. As a result, the system achieves similar BER performance for different values of $|\rho_{12}|$, as illustrated in Fig. 9.

C. Time-varying Correlations

In this sub-section, we present the simulation result for the case of time-varying correlations with $T_\rho < T_b$. As discussed in Subsection V-B, we have to deal with both the time-varying channel and the "virtually change" in the jamming channels due to the change over time of the correlations between transmitted jamming signals. To deal with those issues, we use the protocol illustrated in Fig. 5 and Algorithm 2 with $N_{\mathrm{sf}} = 5$, and $\gamma_{\mathrm{r}} = 0.05$. Note that in this simulation, the

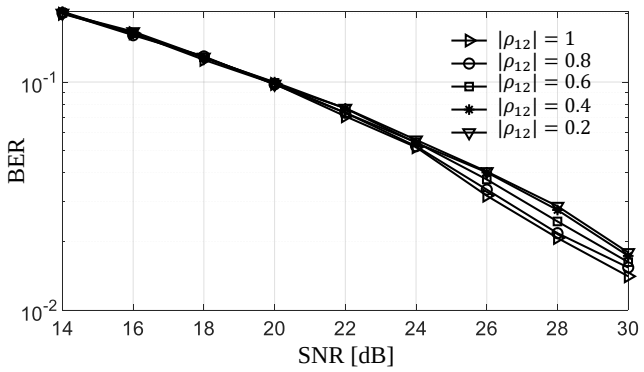

Fig. 9: BER performance when $|\rho_{12}|$ is unchanged.

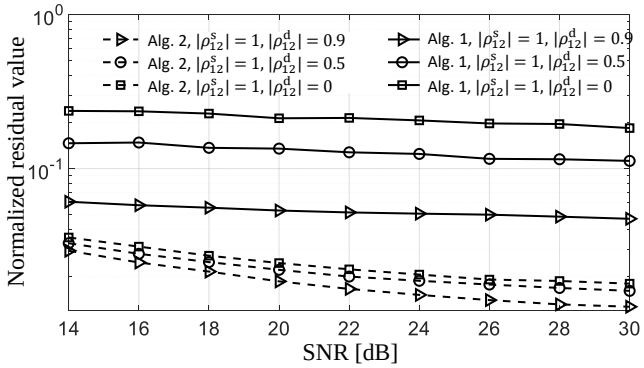

Fig. 10: r_{J} values for different values of $|\rho_{12}^{\mathrm{s}}|$ and $|\rho_{12}^{\mathrm{d}}|$.

correlation between transmitted jamming signals is assumed to change linearly. Therefore, the changes from $|\rho_{12}^{\mathrm{s}}|$ into $|\rho_{12}^{\mathrm{d}}|$ over one frame is equally divided into $N_{\mathrm{sf}} = 5$ changes over each sub-frame.

Fig. 10 illustrates the values of r_{J} for different scenarios of the time-varying correlations between transmitted jamming signals. As can be seen, there are large jamming residual values for the system using the protocol in Alg. 1 and Fig. 4. It means the above protocol is unable to catch "virtually change" in the jamming channels, caused by the change in the correlations between transmitted jamming signals. Another phenomenon is that the jamming residual becomes larger with the larger difference between $|\rho_{12}^{\mathrm{s}}|$ and $|\rho_{12}^{\mathrm{d}}|$. That is because a larger difference between $|\rho_{12}^{\mathrm{s}}|$ and $|\rho_{12}^{\mathrm{d}}|$ results in larger elements of the "virtual change" factor $\mathbf{F}$. On the other hand, the system using the protocol in Alg. 2 and Fig. 5 has successfully caught up the "virtually change" in the jamming channels, results in a much smaller jamming residual.

Fig. 11 compares the BER performance of the system using protocol in Alg. 1 and Fig. 4 to that of the protocol in Alg. 2 and Fig. 5 for different scenarios of the time-varying correlations mentioned above. As can be seen, the system using the protocol in Alg. 1 and Fig. 4 has high BER values, because the jamming signals are not effectively nullified. On the other hand, the system using the protocol in Alg. 2 and Fig. 5 successfully nullify the jamming signals, result in BER results similar to that of the system using the protocol in Alg.1 and Fig. 4 for the case of uncorrelated jamming signals.

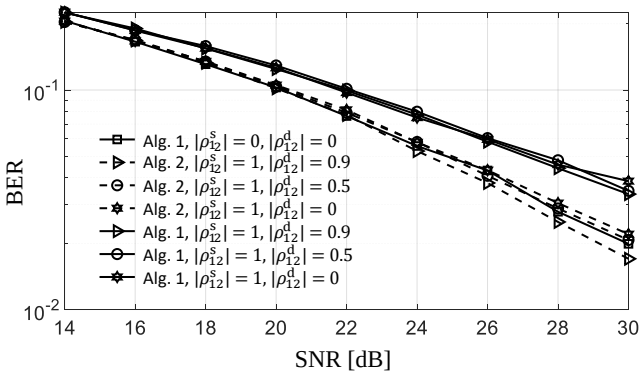

Fig. 11: BER for different values of $|\rho_{12}^{\mathrm{s}}|$ and $|\rho_{12}^{\mathrm{d}}|$.

VII. Conclusion and Future Work

We investigated the impact of non-zero and time-varying correlations between transmitted jamming signals on the jamming channels' left nullspace estimation and received jamming signals nullification. We proposed the technique to effectively suppress the received jamming signals for different levels of correlations between transmitted jamming signals. Monte Carlo simulation results show that our techniques can nullify the jamming signals for different values of the correlations. It is worth noting that the techniques proposed in this manuscript can be extended to a wideband OFDM system with frequency-selective multipath channels by applying the technique to, e.g., each sub-carrier of the OFDM system. The future research problem is to design the parameters of the communication protocol analytically.

Appendix A
Proof of Theorem 1

Let $\mathbf{X}_{\mathrm{J}}^{\mathrm{s}}$ and $\mathbf{N}$ be sample sets containing N_{s} samples of $\mathbf{x}_{\mathrm{J}}^{\mathrm{s}}$ and noise $\mathbf{n}$, respectively. Because $\mathbf{x}_{\mathrm{J}}^{\mathrm{s}} \sim \mathcal{CF}(\boldsymbol{\mu}_{\mathrm{J}}^{\mathrm{s}}, \boldsymbol{\Sigma}_{\mathrm{J}}^{\mathrm{s}})$, we have $\mathbb{E}(\mathbf{X}_{\mathrm{J}}^{\mathrm{s}}) = \boldsymbol{\mu}_{\mathrm{J}}^{\mathrm{s}}$ and $\mathbb{E}(\mathbf{X}_{\mathrm{J}}^{\mathrm{s}}(\mathbf{X}_{\mathrm{J}}^{\mathrm{s}})^H) = N_{\mathrm{s}}\boldsymbol{\Sigma}_{\mathrm{J}}^{\mathrm{s}}$.

Then, recalling that $\mathbf{Z}_k$ is deterministic, we have

$$
\begin{aligned}
\mathbb{E}(\mathbf{R}_{\mathrm{J}_k}^{\mathrm{s}}) &= \mathbb{E}\left(\frac{1}{N_{\mathrm{s}}}\mathbf{Y}_{\mathrm{J}_k}^{\mathrm{s}}(\mathbf{Y}_{\mathrm{J}_k}^{\mathrm{s}})^H\right) \\
&= \frac{1}{N_{\mathrm{s}}}\mathbb{E}\left((\mathbf{Z}_k\mathbf{X}_{\mathrm{J}}^{\mathrm{s}} + \mathbf{N})(\mathbf{Z}_k\mathbf{X}_{\mathrm{J}}^{\mathrm{s}} + \mathbf{N})^H\right) \\
&= \frac{1}{N_{\mathrm{s}}}\mathbb{E}\left(\mathbf{Z}_k\mathbf{X}_{\mathrm{J}}^{\mathrm{s}}(\mathbf{X}_{\mathrm{J}}^{\mathrm{s}})^H\mathbf{Z}_k^H + \mathbf{N}(\mathbf{X}_{\mathrm{J}}^{\mathrm{s}})^H\mathbf{Z}_k^H + \mathbf{Z}_k\mathbf{X}_{\mathrm{J}}^{\mathrm{s}}\mathbf{N}^H + \mathbf{N}\mathbf{N}^H\right) \\
&= \frac{1}{N_{\mathrm{s}}}\mathbb{E}\left(\mathbf{Z}_k\mathbf{X}_{\mathrm{J}}^{\mathrm{s}}(\mathbf{X}_{\mathrm{J}}^{\mathrm{s}})^H\mathbf{Z}_k^H\right) + \frac{1}{N_{\mathrm{s}}}\mathbb{E}\left(\mathbf{N}(\mathbf{X}_{\mathrm{J}}^{\mathrm{s}})^H\mathbf{Z}_k^H\right) \\
&\quad + \frac{1}{N_{\mathrm{s}}}\mathbb{E}(\mathbf{Z}_k\mathbf{X}_{\mathrm{J}}^{\mathrm{s}}\mathbf{N}^H) + \frac{1}{N_{\mathrm{s}}}\mathbb{E}(\mathbf{N}\mathbf{N}^H) \\
&= \mathbf{Z}_k\boldsymbol{\Sigma}_{\mathrm{J}}^{\mathrm{s}}\mathbf{Z}_k^H + \mathbf{0} + \mathbf{0} + \sigma_n^2\mathbf{I}_{N_k} \\
&= \mathbf{Z}_k\boldsymbol{\Sigma}_{\mathrm{J}}^{\mathrm{s}}\mathbf{Z}_k^H + \sigma_n^2\mathbf{I}_{N_k}
\end{aligned} \tag{16}
$$

Therefore, by the law of large number [33, p. 175] the sample covariance $\mathbf{R}_{\mathrm{J}_k}^{\mathrm{s}}$ converges in probability to $(\mathbf{Z}_k\boldsymbol{\Sigma}_{\mathrm{J}}^{\mathrm{s}}\mathbf{Z}_k^H + \sigma_n^2\mathbf{I}_{N_k})$.

Appendix B
Proof of Theorem 2

Because the receiver uses the covariance matrix of the received jamming signals to estimate $\mathbf{Q}_{\mathrm{s}_k}^{\mathrm{s}}$, we examine the

change from $\mathbf{R}^{\rm s}_{{\rm J}_k}$ to $\mathbf{R}^{\rm d}_{{\rm J}_k}$ due to the change from $\mathbf{\Sigma}^{\rm s}_{\rm J}$ to $\mathbf{\Sigma}^{\rm d}_{\rm J}$. Similar to Section III, we assume the numbers of signal samples are sufficiently large such that the law of large number is applicable. Note that $\mathbf{S}^{\rm s}$ and $\mathbf{S}^{\rm d}$ are diagonal matrices, while $\mathbf{V}^{\rm s}$ is an orthogonal matrix, such that $(\mathbf{V}^{\rm s})^H\mathbf{V}^{\rm s}=\mathbf{I}$, we have,

$$\begin{aligned}
&\mathbf{Z}_k\mathbf{\Sigma}^{\rm d}_{\rm J}\mathbf{Z}_k^H+\sigma_n^2\mathbf{I}_{N_k}\\
&=\mathbf{Z}_k\mathbf{V}^{\rm d}\mathbf{S}^{\rm d}(\mathbf{V}^{\rm d})^H\mathbf{Z}_k^H+\sigma_n^2\mathbf{I}_{N_k}\\
&=\mathbf{Z}_k\mathbf{V}^{\rm d}\sqrt{\mathbf{S}^{\rm d}(\mathbf{S}^{\rm s})^{-1}}\mathbf{S}^{\rm s}\sqrt{\mathbf{S}^{\rm d}(\mathbf{S}^{\rm s})^{-1}}(\mathbf{V}^{\rm d})^H\mathbf{Z}_k^H+\sigma_n^2\mathbf{I}_{N_k}\\
&=\mathbf{Z}_k\mathbf{V}^{\rm d}\sqrt{\mathbf{S}^{\rm d}(\mathbf{S}^{\rm s})^{-1}}(\mathbf{V}^{\rm s})^H\mathbf{V}^{\rm s}\mathbf{S}^{\rm s}(\mathbf{V}^{\rm s})^H\\
&\qquad\times\mathbf{V}^{\rm s}\sqrt{\mathbf{S}^{\rm d}(\mathbf{S}^{\rm s})^{-1}}(\mathbf{V}^{\rm d})^H\mathbf{Z}_k^H+\sigma_n^2\mathbf{I}_{N_k}\\
&=(\mathbf{Z}_k\mathbf{F})\mathbf{V}^{\rm s}\mathbf{S}^{\rm s}(\mathbf{V}^{\rm s})^H(\mathbf{Z}_k\mathbf{F})^H+\sigma_n^2\mathbf{I}_{N_k}\\
&=(\mathbf{Z}_k\mathbf{F})\mathbf{\Sigma}^{\rm s}_{\rm J}(\mathbf{Z}_k\mathbf{F})^H+\sigma_n^2\mathbf{I}_{N_k}.
\end{aligned}$$

Therefore, the change from $\mathbf{\Sigma}^{\rm s}_{\rm J}$ to $\mathbf{\Sigma}^{\rm d}_{\rm J}$ cause a "virtual change" in the jamming channels from $\mathbf{Z}_k$ to $(\mathbf{Z}_k\mathbf{F})$.

abc xyz gsogjsgosjgpsgsipgskgposgs

REFERENCES

[1] K. Grover, A. Lim, and Q. Yang, "Jamming and anti-jamming techniques in wireless networks: a survey," *Int. J. Ad Hoc Ubiquitous Comput.*, vol. 17, no. 4, pp. 197–215, 2014.

[2] Z. Chen, G. Gokeda, and Y. Yu, *Introduction to Direction-of-arrival Estimation*, Norwood, MA, USA, 2010.

[3] R. O. Schmidt, "Multiple emitter location and signal parameter estimation," *IEEE Trans. Antennas Propag.*, vol. 34, no. 3, pp. 276–280, Mar. 1986.

[4] R. Roy and T. Kailath, "ESPRIT-estimation of signal parameters via rotational invariance techniques," *IEEE Trans. Acoust., Speech, Signal Process.*, vol. 37, no. 7, pp. 984–995, 1989.

[5] Y. Hua and T. K. Sarkar, "Matrix pencil method for estimating parameters of exponentially damped/undamped sinusoids in noise," *IEEE Trans. Acoust., Speech, Signal Process.*, vol. 38, no. 5, pp. 814–824, 1990.

[6] A. J. Fenn, *Adaptive antennas and phased arrays for radar and communications*, Boston, MA, USA, 2007.

[7] L. Lu, G. Y. Li, A. L. Swindlehurst, A. Ashikhmin, and R. Zhang, "An overview of massive MIMO: Benefits and challenges," *IEEE J. Sel. Topics Signal Process.*, vol. 8, no. 5, pp. 742–758, 2014.

[8] T. T. Do, E. Björnson, E. G. Larsson, and S. M. Razavizadeh, "Jamming-resistant receivers for the massive MIMO uplink," *IEEE Trans. Inf. Forensics Security*, vol. 13, no. 1, pp. 210–223, 2017.

[9] H. Akhlaghpasand, E. Björnson, and S. M. Razavizadeh, "Jamming suppression in massive MIMO systems," *IEEE Trans. Circuits Syst. II, Exp. Briefs*, vol. 67, no. 1, pp. 182–186, 2019.

[10] ——, "Jamming-robust uplink transmission for spatially correlated massive MIMO systems," *IEEE Trans. Commun.*, vol. 68, no. 6, pp. 3495–3504, 2020.

[11] Q. Yan, H. Zeng, T. Jiang, M. Li, W. Lou, and Y. T. Hou, "Jamming resilient communication using MIMO interference cancellation," *IEEE Trans. Inf. Forensics Security*, vol. 11, no. 7, pp. 1486–1499, 2016.

[12] X. G. Doukopoulos and G. V. Moustakides, "Fast and stable subspace tracking," *IEEE Trans. Signal Process.*, vol. 56, no. 4, pp. 1452–1465, 2008.

[13] J.-F. Yang and M. Kaveh, "Adaptive eigensubspace algorithms for direction or frequency estimation and tracking," *IEEE Trans. Acoust., Speech, Signal Process.*, vol. 36, no. 2, pp. 241–251, 1988.

[14] S. Attallah and K. Abed-Meraim, "Low-cost adaptive algorithm for noise subspace estimation," *Electron. Lett.*, vol. 38, no. 12, pp. 609–611, 2002.

[17] Y. Léost, M. Abdi, R. Richter, and M. Jeschke, "Interference rejection combining in LTE networks," *Bell Labs Tech. J.*, vol. 17, no. 1, pp. 25–49, 2012.

[15] S. Attallah, "The generalized Rayleigh's quotient adaptive noise subspace algorithm: A Householder transformation-based implementation," *IEEE Trans. Circuits Syst. I*, vol. 53, pp. 3–7, 2006.

[16] S. Bartelmaos and K. Abed-Meraim, "Principal and minor subspace tracking: Algorithms & stability analysis," in *Proc. IEEE ICASSP'06*, vol. III, Toulouse, France, May 2006, pp. 560–563.

[18] M. H. Brady, M. Mohseni, and J. M. Cioffi, "Spatially-correlated jamming in gaussian multiple access and broadcast channels," in *Proc. CISS*, Princeton, NY, USA, Mar. 2006, pp. 1635–1639.

[19] J. Gao, S. A. Vorobyov, H. Jiang, and H. V. Poor, "Worst-case jamming on MIMO Gaussian channels," *IEEE Trans. Signal Process.*, vol. 63, no. 21, pp. 5821–5836, 2015.

[20] T.-J. Shan, M. Wax, and T. Kailath, "On spatial smoothing for direction-of-arrival estimation of coherent signals," *IEEE Trans. Acoust., Speech, Signal Process.*, vol. 33, no. 4, pp. 806–811, 1985.

[21] Y. Noam and A. J. Goldsmith, "Blind null-space learning for MIMO underlay cognitive radio with primary user interference adaptation," *IEEE Trans. Wireless Commun.*, vol. 12, no. 4, pp. 1722–1734, 2013.

[22] A. Manolakos, Y. Noam, K. Dimou, and A. J. Goldsmith, "Blind null-space tracking for MIMO underlay cognitive radio networks," in *Proc. Global Commun. Conf.*, 2012, pp. 1223–1229.

[23] W. Su, Z. Safar, M. Olfat, and K. R. Liu, "Obtaining full-diversity space-frequency codes from space-time codes via mapping," *IEEE Trans. Signal Process.*, vol. 51, no. 11, pp. 2905–2916, 2003.

[24] A. Wittneben, "A new bandwidth efficient transmit antenna modulation diversity scheme for linear digital modulation," in *Proc. IEEE Int. Conf. Commun. (ICC)*, May 1993, pp. 1630–1634.

[25] G. Strang, *Introduction to linear algebra*. Wellesley, MA, USA: Wellesley-Cambridge Press, 2016.

[26] G. S. Prabhu and P. M. Shankar, "Simulation of flat fading using matlab for classroom instruction," *IEEE Trans. Educ.*, vol. 45, no. 1, pp. 19–25, 2002.

[27] E. Damosso, L. M. Correia *et al.*, "Digital mobile radio towards future generation systems," Eur. Commission, Brussels, Belgium, Tech. Rep., Apr. 1999.

[28] C. Xiao, Y. R. Zheng, and N. C. Beaulieu, "Novel sum-of-sinusoids simulation models for Rayleigh and Rician fading channels," *IEEE Trans. Wireless Commun.*, vol. 5, no. 12, pp. 3667–3679, 2006.

[29] A. Kekirigoda, K.-P. Hui, Q. Cheng, Z. Lin, A. Zhang, J. Zhang, D. Nguyen, and X. Huang, "Massive MIMO for tactical ad-hoc networks in RF contested environments," in *IEEE/AFCEA Mil. Commun. Conf. (MILCOM)*, 2019.

[30] E. Fishler, M. Grosmann, and H. Messer, "Detection of signals by information theoretic criteria: General asymptotic performance analysis," *IEEE Trans. Signal Process.*, vol. 50, no. 5, pp. 1027–1036, 2002.

[31] J.-J. Van De Beek, O. Edfors, M. Sandell, S. K. Wilson, and P. O. Borjesson, "On channel estimation in OFDM systems," in *Proc. IEEE 45th Veh. Technol. Conf. (VTC)*, Chicago, IL, USA, Jul. 1995, pp. 815–819.

[32] A. Goldsmith, *Wireless communications*. Cambridge, U.K: Cambridge Univ. Press, 2005.

[33] R. A. Johnson and D. W. Wichern, *Applied multivariate statistical analysis*. New Jersey, US: Pearson Prentice Hall, 2007.

[34] P. J. Schreier and L. L. Scharf, *Statistical signal processing of complex-valued data: the theory of improper and noncircular signals*. Cambridge, UK: Cambridge Univ. Press, 2010.

[35] A. S. Lalos, V. Kekatos, and K. Berberidis, "Adaptive conjugate gradient dfes for wideband mimo systems," *IEEE Trans. Signal Process.*, vol. 57, no. 6, pp. 2406–2412, 2009.

[36] J. Choi, H. Yu, and Y. H. Lee, "Adaptive mimo decision feedback equalization for receivers with time-varying channels," *IEEE Trans. Signal Process.*, vol. 53, no. 11, pp. 4295–4303, 2005.

[37] G. H. Golub and C. F. Van Loan, *Computation Matrix*. Baltimore, MD: Johns Hopkins Univ. Press, 2013.

[38] E. S. Sousa, V. M. Jovanovic, and C. Daigneault, "Delay spread measurements for the digital cellular channel in toronto," *IEEE Trans. Veh. Tech-nol.*, vol. 43, no. 4, pp. 837–847, 1994.

[39] D. Tse and P. Viswanath, *Fundamentals of wireless communication*. Cambridge, UK: Cambridge University Press, 2005.